

X-ray magnetic circular dichroism study of uranium/iron multilayers

F. Wilhelm, N. Jaouen, A. Rogalev, and W. G. Stirling*

European Synchrotron Radiation Facility, Boîte Postale 220, F-38043 Grenoble Cedex, France

R. Springell and S. W. Zochowski

Department of Physics and Astronomy, University College London, London WC1E 6BT, United Kingdom

A. M. Beesley, S. D. Brown, and M. F. Thomas

Department of Physics, University of Liverpool, Liverpool L69 7ZE, United Kingdom

G. H. Lander

Institute for Transuranium Elements, European Commission, JRC, Postfach 2340, 76125 Karlsruhe, Germany

S. Langridge

Rutherford Appleton Laboratory, Chilton, Didcot, Oxon OX11 0QX, United Kingdom

R. C. C. Ward and M. R. Wells

Clarendon Laboratory, University of Oxford, Oxford, Oxon OX1 3PU, United Kingdom

(Received 30 March 2006; revised manuscript received 26 January 2007; published 18 July 2007)

X-ray magnetic circular dichroism (XMCD) measurements were performed at the U $M_{4,5}$ edges and Fe K edge on well-defined uranium/iron multilayers with different compositions. The multilayers have layer thicknesses in the range 9–40 Å for uranium and 9–34 Å for iron. At both 10 K and room temperature, the U layers are magnetically polarized in all of the multilayers studied. To deduce the magnetic moment on the uranium from the XMCD results requires assumptions about the magnetic dipole operator $\langle T_z \rangle$ in the analysis, and this is discussed in detail. Given the most likely scenario of strong hybridization between the U $5f$ and Fe $3d$ states, the largest value of the induced U moment is $\sim 0.12\mu_B$, which is located primarily at the interface and oscillates within the uranium layer.

DOI: [10.1103/PhysRevB.76.024425](https://doi.org/10.1103/PhysRevB.76.024425)

PACS number(s): 75.70.Cn, 78.70.Dm, 75.25.+z

I. INTRODUCTION

Magnetic multilayers consisting of ferromagnetic and nonmagnetic elements exhibit many properties of interest for both basic and applied research.¹ These properties are mainly related to the large number of interfaces, which lead to modifications in the properties as compared to those of the bulk materials. The magnetic polarization of the nonmagnetic element is one of the most interesting of these modifications. Such a polarization has been probed in the past for bulk materials only.² However, during the last decade, the development of techniques with element specificity and monolayer sensitivity, such as x-ray magnetic circular dichroism (XMCD),³ permits a more systematic study of induced ferromagnetism in thin multilayer structures. To date, most efforts have been focused on the induced magnetic moments of the $3d$, $4d$, and $5d$ transition-metal series,⁴ whereas the induced magnetism of $5f$ elements in magnetic multilayers is still largely unexplored. Indeed, the combination of a soft magnetic element like iron and an element that possesses a large spin-orbit coupling, such as uranium, may give rise to interesting and unusual magnetic properties. Moreover, the magnetism of uranium in bulk compounds exhibits a rich variety of properties, ranging from Pauli paramagnetism, through localized and itinerant magnetism, to heavy-fermion behavior and superconductivity.⁵

The element uranium is nonmagnetic, but many uranium compounds show strong magnetic behavior. The interactions

governing these properties are the Coulomb and exchange interactions, the crystal field, the spin-orbit coupling, and hybridization. These, along with the large orbital moment of the $5f$ electrons, which is larger in magnitude than the spin moment, give rise to strong anisotropies of potential interest for technological applications. Uranium-based multilayers could, at least in theory, be an alternative to existing transition-metal-based multilayers. However, very few studies have been reported on uranium-based multilayers. A ground-breaking study of UAs/Co multilayers⁶ showed that the uranium atom could carry a finite magnetic moment induced through exchange coupling with the Co layers. This was quantified later, using XMCD, and a linear relation between the polar Kerr rotation and the U $5f$ magnetic moment was found, demonstrating that the (small) U $5f$ moment is responsible for the large magneto-optical effects.⁷

The experiments on the UAs/Co multilayers^{6,7} started with an amorphous *ferromagnetic* material as one component. Such ferromagnetism is recognized as being produced in actinide materials by well separating the actinide ions, so that they exceed the critical Hill interatomic distance of ~ 3.2 Å for uranium.⁵ The situation when using elemental uranium, as in the present studies, is different, since the U-U spacing is then less than the Hill limit, so magnetic behavior can be induced only by a modification of the structure at the interface or by hybridization with the Fe $3d$ electrons. To observe any effect on the U sites, which will certainly be small, requires an element-specific technique. A preliminary

TABLE I. Structural parameters obtained by fitting the neutron reflectivity (Ref. 9) and magnetic moments per Fe atom measured by SQUID magnetometry (Refs. 10 and 11) of the U/Fe multilayers. U and Fe layer thicknesses, t_U and t_{Fe} , respectively, and the bilayer repeats n are indicated in the three first columns whereas the last column shows the magnetic moments per Fe atom in units of μ_B .

Sample	t_U (± 2) (Å)	t_{Fe} (± 2) (Å)	Bilayer repeats	SQUID
				magnetic moment/Fe atom (μ_B)
SN71	9	34	30	1.39 ± 0.09
S3.6	18	34	100	1.79 ± 0.05
SN72	23	17	10	0.18 ± 0.05
S2.9	26	29	30	1.17 ± 0.05
SN75	32	30	30	1.23 ± 0.08
S3.4	40	9	100	0.24 ± 0.17

report using x-ray resonant reflectivity⁸ gave a signal associated with the U atoms, as evidenced by a signal at the U M_4 edge, on one multilayer sample. However, no conclusions could be drawn as to the magnitude of the effect or details of the profile within the uranium layer. The present paper follows up that preliminary report with a systematic study of a number of samples using XMCD. This has allowed both the magnitudes and profile of the induced moments across the uranium layers to be deduced.

II. EXPERIMENT

Two series of U/Fe multilayer samples were used in this study. The first samples (series ‘‘S’’) were grown in a dedicated two-gun dc sputtering facility, which could be baked to give a base vacuum of 2×10^{-10} mbar. The sputtering system had an ambient-temperature rotating mount for two substrates. Deposition from high-purity targets (>99.9%) was made at calibrated rates of approximately 3 \AA/s onto glass substrates in an Ar pressure of 5×10^{-3} mbar. Details of the preparation and the structural and magnetic characterization of these multilayers can be found in the two articles by Beesley *et al.*^{9,10}

The second series of U/Fe multilayers, listed as ‘‘SN,’’ was produced also by UHV sputtering but using a newly developed growth facility configured with three individually shuttered dc sources. These multilayers were deposited onto single-crystal sapphire substrates at $\approx 1 \text{ \AA/s}$ in an Ar pressure of 5×10^{-3} mbar. Niobium was employed for both buffer and capping. Table I lists the individual layer thicknesses obtained from the x-ray reflectivity data, using standard programs.^{9,12} The number of bilayer repeats and the magnetic moment per Fe atom were deduced using superconducting quantum interference device (SQUID) magnetometry and polarized neutron reflectivity.^{10,11}

The XMCD measurements reported here were carried out on the beamline ID12, which is dedicated to polarization-dependent spectroscopies, at the European Synchrotron Radiation Facility (ESRF) in Grenoble, France. A detailed de-

scription of the beamline can be found in Ref. 13. The x-ray absorption near-edge spectrum (XANES) at both the U M_4 and M_5 edges and the Fe K edge were recorded in a back-scattering geometry with a grazing incidence angle of about 15° . The x-ray source for the U M edges is a hybrid electromagnet–permanent magnet helical undulator, which allows XMCD spectra to be obtained by flipping the helicity of the circularly polarized x-ray beam at each energy. Moreover, to ensure that the measured XMCD spectra are free of any experimental artifact, the data were collected for both directions of the external applied magnetic field (parallel and antiparallel to the incoming x-ray beam). The applied magnetic field, up to 1 T, was produced by a superconducting cryomagnet. The measurements were performed at 10 K and at room temperature for all samples. At the energies of the U M_5 (3.55 keV) and M_4 edges (3.73 keV), the Bragg angle of the double Si(111) crystal monochromator is above the Brewster angle; therefore the degree of circular polarization of the monochromatic beam is reduced to 35% and 45%, respectively. The x-ray source for the Fe K edge (7.11 keV) was an Apple-II-type helical undulator. At this energy, the degree of circular polarization of the monochromatic beam is about 90%.

The XMCD spectra were obtained as the difference between consecutive XANES scans recorded with opposite helicities of the incoming circularly polarized x-ray beam. Absorption spectra for U and Fe were measured in the fluorescence yield mode, using Si photodiodes. This mode is the easiest method to use in the presence of a magnetic field; nevertheless, self-absorption corrections to the measured fluorescence spectrum in the case of U M edges are required to obtain the absorption coefficient. The experimental procedure to obtain the absorption coefficient was the following. First, the U M_4 and M_5 edge jumps were normalized to unity. Second, the corresponding XMCD spectra were corrected for the incomplete energy-dependent degree of circular polarization. Third, the corresponding absorption spectra for 100% right and left circularly polarized x-ray beams were corrected for self-absorption, taking into account the structure of the multilayer (individual thicknesses of the U and Fe layers, their respective bulk densities, the number of repetitions, the buffer and substrate, and capping layers), the angle of incidence of the x-ray beam, and finally the solid angle of the detector.¹⁴ The self-absorption corrections can be used with confidence as a measure of the absorption coefficient at the $M_{4,5}$ edges of U, since the spin-orbit coupling at these edges is large. To ensure the accuracy of the self-absorption corrections, the absorption spectra taken at grazing ($\sim 15^\circ$) and at normal incidence were compared; after correction, nearly identical absorption spectra for each M_4 and M_5 edge were obtained. Finally, the edge-jump intensity ratio $M_5:M_4$ was normalized to 1:2/3 according to the statistical edge jump ratio (defined as the ratio between the occupation numbers for the two spin-orbit-split core levels $j=3/2$ and $5/2$). The experimental edge jump ratios for all samples were found to be within less than 10% of the statistical one. Regarding the Fe K edge, the spectra were also corrected for self-absorption after normalization of the edge jump to unity. The fluorescence corrections at the Fe K edge were made using the same experimental configuration and multilayer structure as for the

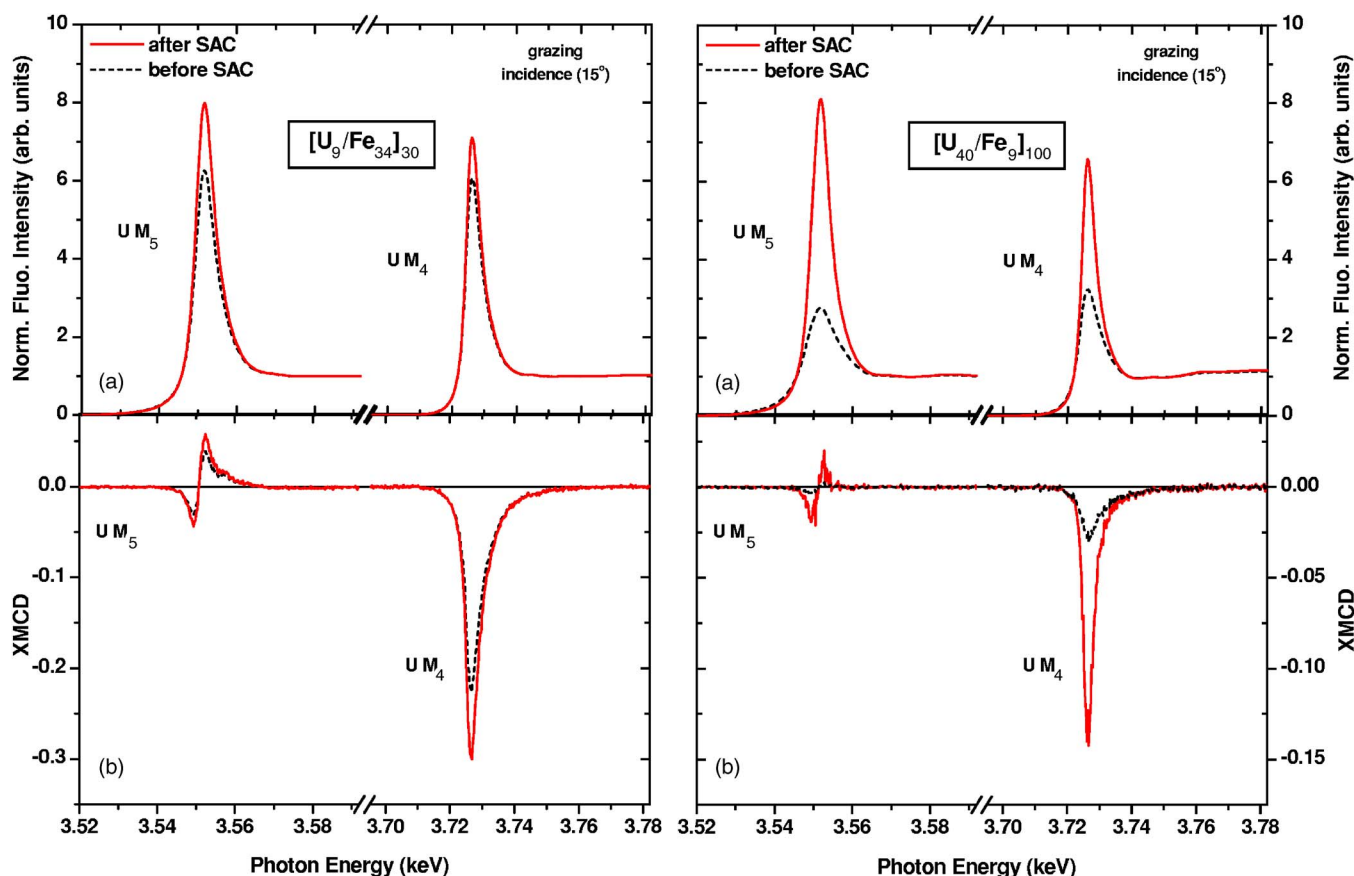


FIG. 1. (Color online) Normalized $M_{4,5}$ edges of U XANES (a) and XMCD (b) spectra before (dashed black line) and after (solid red line) self-absorption corrections (SAC) for a multilayer containing a small total U thickness (270 Å) as in $[U_9/Fe_{34}]_{30}$ (left panel) and for a multilayer containing a large total U thickness (4000 Å) as in $[U_{40}/Fe_9]_{100}$ (right panel) measured at 10 K and 0.5 T, for grazing incidence.

U M edges. Figure 1 illustrates the self-absorption corrections at the U M edges for U/Fe multilayers with thin and thick U layers. The effect of the corrections is to enhance the intensity of the white lines with a different factor for the two edges. It is clear from this example that corrections to the intensity of the XMCD signal are much greater for samples with thick uranium layers. However, we have to emphasize that, since the XMCD area at the M_5 edge is less than 10% of that at the M_4 edge, the measured expectation values will only weakly depend (of the order of a few percent) on these normalizations and corrections.

III. RESULTS AND DISCUSSION

This section is divided into two parts. The first part will deal with the XANES and XMCD measured at the K edge of Fe, whereas the second part deals with the U $5f$ induced magnetic polarization and its dependence on the Fe layer thickness.

A. Fe K edge XANES and XMCD

1. Fe K edge XANES

In Fig. 2(a) we present the normalized and averaged Fe K edge XANES for left and right circularly polarized x rays measured by fluorescence yield for several representative

U/Fe multilayers for different Fe and U thickness. At first sight, all the Fe K edge spectra seem to be similar in shape, independent of the Fe and U thickness. However, on closer inspection, the XANES spectra fall into two groups, corresponding to U/Fe multilayers with thick and thin Fe layers, with small, but significant, differences in their spectral shape. For thick Fe layers (30 Å and above), the XANES spectrum corresponds to that of textured α -Fe (bcc) with a characteristic small shoulder located at 7.123 keV [marked as feature 2 in Fig. 2(b)]. For thin Fe layers (17 Å and less), small differences are observed in the spectral shape of the XANES spectrum compared to bcc Fe. First, the intensity of the pre-edge feature is slightly stronger (feature 1), and, second, the typical post-edge shoulder (feature 2) present in bcc Fe is attenuated. Moreover, the maximum at the edge (feature 3) is located about 2 eV lower than that for a thick Fe layer. Finally, the maximum of the first extended x-ray-absorption fine structure wiggles (feature 4) is at higher energy for the thinner Fe layers. These differences are even more pronounced for the sample with the thinnest Fe layers (9 Å). In the last case, small changes in the charge density of states due to lattice distortions could also be present. Indeed, previous structural characterization by high-angle x-ray diffraction has shown that the iron lattice parameter is larger than the bulk value for smaller Fe thicknesses.⁹ However, the XANES signal for samples with thin Fe layers strongly re-

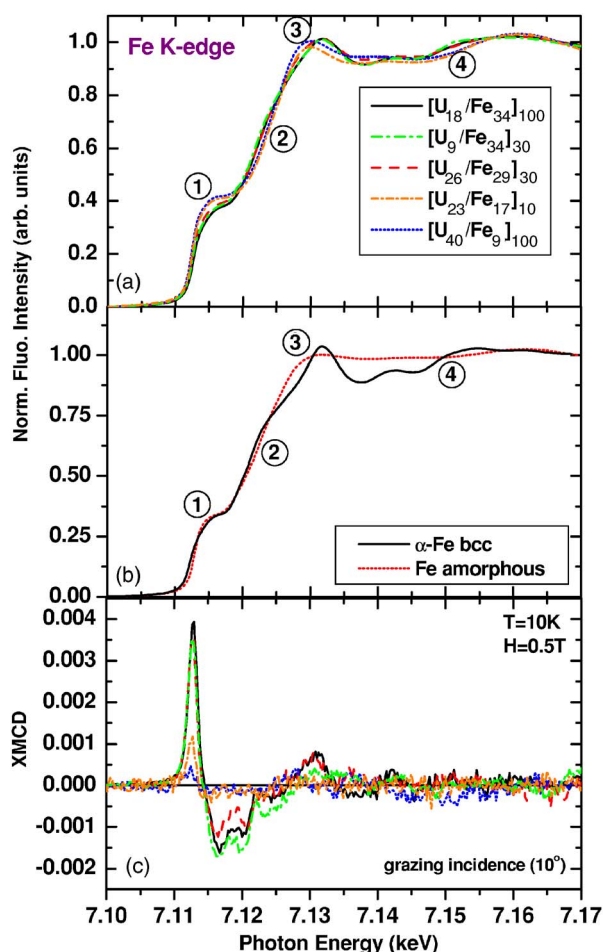


FIG. 2. (Color online) Normalized XANES (a) and XMCD (c) spectra measured at the K edge of Fe in U/Fe multilayers at 10 K and 0.5 T, for grazing incidence. A series of multilayers with decreasing Fe thickness independent of the U thickness has been selected for illustration. For comparison, normalized XANES (b) spectra measured at the K edge of Fe for an α -Fe bcc thin foil and a typical amorphous Fe sample are presented.

sembles that of amorphous iron, the characteristics of which are nearly identical to that presented here;¹⁵ namely, the absence of the shoulder (feature 2) and a lower energy for the edge maximum (feature 3) [see Fig. 2(b)]. Similar conclusions concerning the presence of amorphous iron were reached on the basis of the Mössbauer spectroscopy measurements on the same U/Fe multilayers.^{9,10} The amorphous Fe contribution appears to be present in all U/Fe multilayers, independent of the U thickness. We conclude that, in the XANES measurements, the amorphous Fe contribution is more observable for thinner Fe thicknesses since the contribution of crystalline bcc Fe is relatively less. Moreover, this implies that the amorphous (or poor crystallinity) Fe is mainly located at the interfaces (U on Fe, or Fe on U) since it is more pronounced for small thicknesses. The precise location cannot be determined from these observations.

2. Fe K edge XMCD

We now turn to the corresponding XMCD spectra, which are shown in Fig. 2(c). All the XMCD spectra have been

taken with the samples magnetically saturated in plane under 0.5 T magnetic field at 10 K. The XMCD spectra are identical in shape and correspond well to the spectrum of bulk bcc Fe, independent of the U or Fe layer thickness. Only the amplitude changes as a function of the Fe layer thickness. The maximum XMCD signal decreases with the Fe thickness from 0.4% down to nearly zero for the thinnest Fe layers. Let us now recall the origin of the dichroism effect at the K edge. It was first pointed out by Gotsis and Strange¹⁶ and Brooks and Johansson¹⁷ that the K edge XMCD spectrum reflects the orbital polarization of the p states in the differential form $d\langle L_z \rangle / dE$ (where $\langle L_z \rangle$ is the ground state expectation value of the z component of the $4p$ orbital magnetic moment). In its integral form, the XMCD at the K edge is then a measure of the orbital magnetism, averaged over the layers, of the $4p$ shell of Fe (considering only dipolar transitions). This leads to a rather simple and straightforward interpretation of the Fe XMCD spectrum at the K edge.^{18,19} Due to the small exchange splitting of the initial $1s$ core states, only the exchange and spin-orbit splitting of the final $4p$ states are responsible for the observed dichroism at the Fe K edge. For this reason the dichroism is found to be small. The orbital polarization in the p symmetric states may be induced by spin polarization through the spin-orbit interaction, and also by the orbital polarization at neighboring sites through hybridization. However, these contributions lead to different “signatures” in the XMCD spectral shape,²⁰ if one neglects allowed quadrupolar transitions. Since the XMCD spectral shapes do not change with thickness, whereas the thinnest Fe layers have a significant fraction of amorphous iron, we conclude that the amorphous Fe is nonmagnetic, as suggested by earlier Mössbauer measurements.^{9,10} Indeed, the K edge XMCD of ferromagnetic amorphous Fe has a completely different shape, consisting mainly of a negative lobe.²¹

3. Possibility of formation of a U-Fe intermetallic alloy

We have also considered the possibility of the formation of U-Fe intermetallic alloys or compounds; the only such compound known to be ferromagnetic is UFe_2 . Below the Curie temperature (T_C) of 160 K, UFe_2 is a ferromagnet with a magnetic moment of $1.16\mu_B$ per formula unit. Moreover, it has a low magnetic anisotropy similar to that of pure Fe,^{22,23} and the net magnetization of UFe_2 is entirely attributable to the Fe atoms.²⁴ In Fig. 3, we present XANES and XMCD spectra recorded at the Fe K edge for a UFe_2 single crystal and for a $\text{U}_{26}/\text{Fe}_{29}$ multilayer. We note that the intensity of the pre-edge feature (at 7.115 keV) is the same in UFe_2 as that of the U/Fe multilayer with thick Fe layers. Despite that, clear differences in the spectral shape are observed in the XANES. The pre-edge structure is completely different since it shows a clear dip on the high-energy side (~ 7.117 keV) in the case of UFe_2 , which is not observed for any U/Fe multilayer. Finally, the maximum at the edge in UFe_2 is located about 3.5 eV lower than that of any multilayer. Thus, from the XANES spectra of the multilayers, there is no indication of an appreciable amount of UFe_2 secondary phases at the interfaces of the U/Fe multilayers studied.

The absence of any appreciable quantity of UFe_2 is confirmed by the XMCD signal, also shown in Fig. 3. In the case

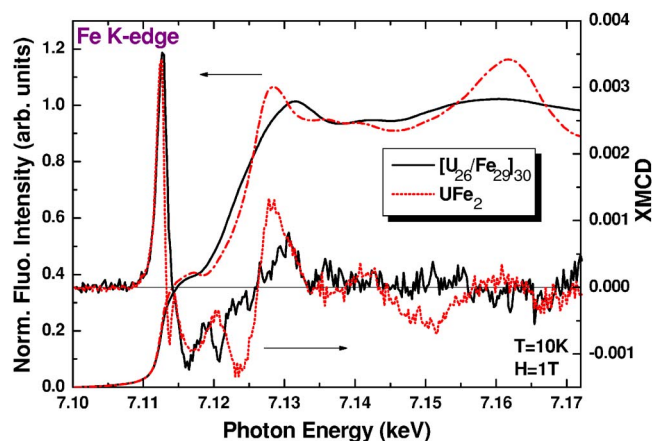


FIG. 3. (Color online) Comparison of XANES (left scale) and XMCD (right scale) spectra measured at the K edge of Fe for $[U_{26}/Fe_{29}]_{30}$ (solid black line) and UFe_2 single crystal (broken red line) at 10 K and 1 T.

of UFe_2 , the XMCD signal located at the pre-edge (~ 7.113 keV) consists of one strong positive peak and a small negative peak on the high-energy side. For the U/Fe multilayers, this negative peak is absent and only one strong positive XMCD peak is observed. Similarly, such negative peaks as found in UFe_2 are absent in other Fe-based magnetic multilayers, e.g., Gd/Fe multilayers.²⁵

In summary, from the above considerations of the XANES and XMCD spectra, we conclude that there is no significant presence of UFe_2 in the multilayers.

4. Dependence of the XMCD signal intensity on the Fe layer thickness

We shall now consider the maximum of the XMCD signal intensity as a function of the Fe layer thickness in the U/Fe multilayers (Fig. 4). We observe that the signal increases rapidly as a function of the Fe thickness but does not seem to saturate. Indeed, pure bulk bcc Fe has a maximum dichroism

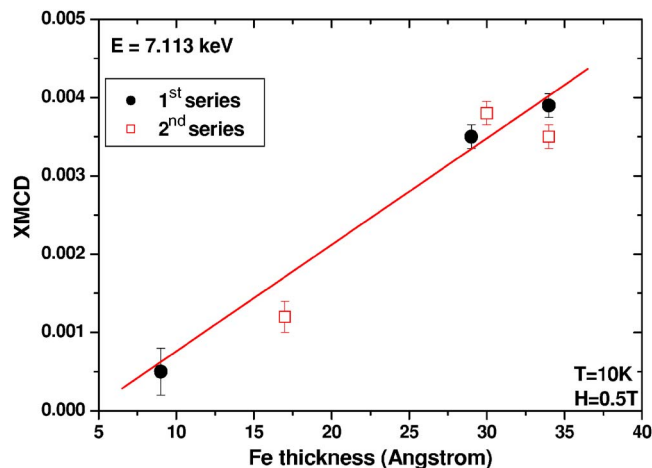


FIG. 4. (Color online) Maximum XMCD signal intensity measured at the K pre-edge of Fe versus the thickness of Fe layers in the U/Fe multilayers. The straight line is a linear fit.

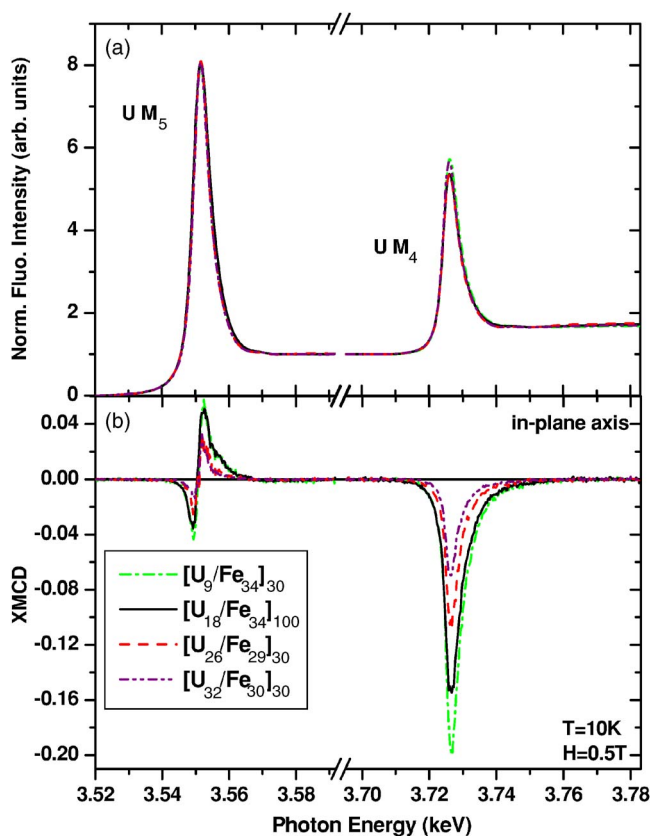


FIG. 5. (Color online) Normalized XANES (a) and XMCD (b) spectra measured at the $M_{4,5}$ edges of U in U/Fe multilayers at 10 K and 0.5 T for grazing incidence. A series of multilayers with nearly constant Fe thickness (~ 32 Å) and increasing U thickness was selected for illustration.

intensity of order of 0.005 compared to the edge jump. The change of signal as a function of Fe thickness shown in Fig. 4 follows the average magnetic moment per Fe atom obtained from polarized neutron reflectometry and SQUID magnetometry (see Fig. 5 in Ref. 10) on the same U/Fe multilayer samples. The magnetic moment of Fe is observed to saturate for a Fe thickness above 60 Å. Moreover, the Fe XMCD intensity appears to depend only on the Fe layer thickness independent of the U layer thickness. In Fig. 4, we present results for two different sets of U/Fe multilayers, prepared separately under different growth conditions. They show the same behavior, thus confirming the proportionality suggested.

B. U $M_{4,5}$ edge XANES and XMCD

1. U $M_{4,5}$ edge XANES

We now present results on the U $5f$ magnetism of these U/Fe multilayers. In Fig. 5(a), we show the normalized and averaged U M_4 and M_5 edge XANES for left and right circularly polarized x rays, measured by fluorescence yield, after self-absorption corrections, for several representative U/Fe multilayers with different U thicknesses while keeping the Fe thickness nearly constant. Contrary to the situation at the Fe K edge, all the XANES spectra at both the M_4 and M_5

edges are similar in amplitude and in their spectral shape, independent of the Fe and U thickness [Figs. 1(a) and 5(a)]. We recall that the M_4 (M_5) edge corresponds to $3d_{3/2}$ ($3d_{5/2}$) $\rightarrow 5f$ transitions. Because of the electric dipole selection rules, the M_4 absorption signal is proportional to the number of $5f_{5/2}$ holes, whereas the M_5 absorption signal depends mainly on the number of $5f_{7/2}$ holes and to a lesser extent on the number of $5f_{5/2}$ holes.^{26–29} Since only small differences are observed, the valence state of the U atoms evidently seems not to change appreciably as a function of U or Fe thickness. To investigate in more detail the nature of the $5f$ electronic states, the spin-orbit sum rule³⁰ is a useful tool. This sum rule is well adapted to probe the $5f$ spin-orbit interaction in the actinides. Furthermore, a connection between the spin-orbit expectation value and the degree of $5f$ localization via the branching ratio has been established. By measuring the branching ratio and comparing it with the theoretically derived angular-momentum coupling of the $5f$ states gives the possibility to define the range of $5f$ occupation number in cases where the f count is not precisely known.^{30–32} For the $d \rightarrow f$ transitions, the spin-orbit sum rule gives the relation

$$\frac{\langle w^{110} \rangle}{n_h^{5f}} - \Delta = -\frac{5}{2} \left(B - \frac{3}{5} \right) \quad (1)$$

where $\langle w^{110} \rangle$ is the expectation value of the angular part of the $5f$ spin-orbit operator, n_h^{5f} is the number of $5f$ holes, B is the branching ratio, and Δ is a small correction term to this sum rule. The correction term Δ in case of the $N_{4,5}$ edges of U is approximately 5% regarding the spin-orbit expectation value per hole $\langle w^{110} \rangle / n_h^{5f}$.³⁰ In the case of the $M_{4,5}$ edges of U, Δ is expected to be smaller since it is proportional to the ratio between the core-valence exchange interaction and the energy splitting between the white lines, and this quantity is larger for the $M_{4,5}$ edges compared to the $N_{4,5}$ edges. Therefore we neglect this correction term Δ . The branching ratio B for the $3d \rightarrow 5f$ transition of U is experimentally determined as

$$B = A_{5/2} / (A_{5/2} + A_{3/2}), \quad (2)$$

where $A_{5/2}$ and $A_{3/2}$ are the integrated areas under the white lines of the $3d_{5/2}$ (M_5 edge) and $3d_{3/2}$ (M_4 edge) peaks, respectively, after subtraction of the continuum, modeled by an arctan function. In Table II are listed the experimental branching ratios for all the U/Fe multilayers. For comparison, we have also shown the value B of α -U metal taken from Ref. 30. Since the analysis (normalization and self-absorption corrections) procedure to obtain the branching ratio is the same for all samples studied, the relative experimental error bar should be in the order of a few percent. The absolute error bar would be larger if one compares B values obtained using different spectroscopic tools.³⁰ The values of B can then be converted to $\langle w^{110} \rangle / n_h^{5f}$. The spin-orbit expectation value can be expressed in the number of holes $n_h^{7/2}$ and $n_h^{5/2}$ in the $5f^{7/2}$ and $5f^{5/2}$ levels, respectively,

$$\langle w^{110} \rangle = n_h^{7/2} - \frac{4}{3} n_h^{5/2} \quad (3)$$

with the relation

$$n_h^{5f} = n_h^{5/2} + n_h^{7/2} = n_e^{5f} - 14, \quad (4)$$

where n_e^{5f} is the occupation of the $5f$ band. When we examine the B values for the different U/Fe multilayers, we observe that they oscillate as a function of the U thickness. This oscillation is more accentuated when it is converted into the spin-orbit expectation value per hole $\langle w^{110} \rangle / n_h^{5f}$. For the smallest U thickness (U₉/Fe₃₄), the spin-orbit expectation value per hole is -0.142 , whereas it becomes larger in an oscillatory way down to -0.215 for the thickest U layer (U₄₀/Fe₉), which could be considered from the electronic perspective as close to bulk α -U. Indeed, the spin-orbit expectation value per hole is nearly identical to that of α -U metal.³⁰ As previously discussed^{30–33} in connection with Fig. 2 of Ref. 30, all the values for the U/Fe multilayers fall near the LS coupling curve. We emphasize that this study, which is based on the M edges of U, arrives at a similar conclusion as Ref. 31, which considers the N edges of U. The result is to suggest that the $5f$ electron count is between 2 and 3, as expected, with the higher electron count corresponding to the situation for thicker U layers. Using the spin-orbit sum rule, we found that the number of $5f$ electrons oscillates between $n_e^{5f} \approx 2$ for the thinnest U layer (U₉/Fe₃₄) and $n_e^{5f} \approx 3$ for the thickest U layer (U₄₀/Fe₉).

2. U $M_{4,5}$ edge XMCD

In Fig. 5(b), we show the XMCD recorded at the U $M_{4,5}$ edges at 10 K and with a 0.5 T applied magnetic field. The existence of the XMCD signal implies that the uranium atoms (averaged over each layer) carry an induced magnetic moment. The XMCD spectra are similar in shape, with only their amplitudes depending on the thickness of U and Fe. We observe that the U M_4 XMCD signal consists of a nearly symmetric negative peak that has no distinct structure. Such a peak is characteristic of the U M_4 edge of uranium compounds.^{26,27} The XMCD signal at the U M_5 edge has a slightly asymmetric (S) shape with both negative and positive peaks. The M_4 dichroism signal is more than four times larger than that at the M_5 edge. More details regarding the origin of the XMCD shape at the U M_5 and M_4 edges can be found in Refs. 26–29. At this point, as discussed in Ref. 26, it is important to recall that these XMCD shapes, especially at the M_5 edge, agree well with calculated ones for both the $n_e^{5f} = 2$ and 3 electronic configurations when the interaction of the uranium $5f$ electrons with their environment is taken into account. Further, it is important to note that the shape of the U M_5 XMCD signal observed here is different from that found for U in UAs/Co multilayers⁷ or in polycrystalline UFe₂.²⁴ Indeed, the XMCD signal at the U M_5 edge of UFe₂ presents a strongly asymmetric S shape, which consists of a strong negative peak and a weak positive peak. Since the shape is completely different from that of our XMCD signal, one can reasonably conclude that no secondary phase of UFe₂ is formed at the U/Fe interfaces in the multilayer, in-

TABLE II. Branching ratio (B), spin-orbit expectation value per hole [Eq. (1)], and induced U $5f$ orbital, spin, and total magnetic moment contribution in units of μ_B for a series of U/Fe multilayers deduced from XMCD measurements performed at 10 K and 1 T using the sum rules assuming different $5f$ contributions. The experimental ratio of orbital to spin magnetic moment should be compared to the theoretical values -2.54 and -3.36 for the f^3 and f^2 configurations, respectively. The induced U $5f$ magnetic moments are tabulated for two cases; including the $\langle T_Z \rangle$ term, and assuming $\langle T_Z \rangle = 0$. Experimental error bars in the values of the spin and orbital moments are negligible compared to the application and validity of the sum rules, which are commonly estimated to be of order 15%, but these affect only the absolute values, not the ratios. The final column has error bars of $\sim 10\%$. XAS indicates X-ray absorption spectroscopy and EELS electron energy-loss spectroscopy.

Sample	B	$\frac{\langle w^{110} \rangle - \Delta}{n_h}$	$\langle T_Z \rangle$	Configuration	$\mu_L(U^{5f})$ $\pm 0.01 (\mu_B)$	$\mu_S(U^{5f})$ $\pm 0.01 (\mu_B)$	$\mu (U^{5f})$ $\pm 0.02 (\mu_B)$	$\mu_L(U^{5f})/\mu_S(U^{5f})$
SN71 [U ₉ /Fe ₃₄] ₃₀	0.657	-0.142	=0	$5f^3$	0.17	-0.295	-0.125	-0.58
				$5f^2$	0.185	-0.32	-0.135	-0.58
			$\neq 0$	$5f^3$	0.17	-0.10	0.07	-1.66
				$5f^2$	0.185	-0.07	0.11	-2.60
S3.6 [U ₁₈ /Fe ₃₄] ₁₀₀	0.683	-0.207	=0	$5f^3$	0.135	-0.25	-0.115	-0.54
				$5f^2$	0.145	-0.275	-0.13	-0.54
			$\neq 0$	$5f^3$	0.135	-0.09	0.045	-1.53
				$5f^2$	0.145	-0.06	0.085	-2.41
S2.9 [U ₂₆ /Fe ₂₉] ₃₀	0.675	-0.187	=0	$5f^3$	0.09	-0.15	-0.06	-0.595
				$5f^2$	0.095	-0.165	-0.07	-0.595
			$\neq 0$	$5f^3$	0.09	-0.05	0.035	-1.71
				$5f^2$	0.095	-0.035	0.06	-2.69
SN75 [U ₃₂ /Fe ₃₀] ₃₀	0.656	-0.140	=0	$5f^3$	0.05	-0.090	-0.040	-0.54
				$5f^2$	0.054	-0.10	-0.046	-0.54
			$\neq 0$	$5f^3$	0.05	-0.032	0.018	-1.54
				$5f^2$	0.054	-0.023	0.029	-2.41
S3.4 [U ₄₀ /Fe ₉] ₁₀₀	0.686	-0.215	=0	$5f^3$	0.07	-0.095	-0.025	-0.73
				$5f^2$	0.08	-0.105	-0.025	-0.73
			$\neq 0$	$5f^3$	0.07	-0.035	0.035	-2.09
				$5f^2$	0.08	-0.025	0.055	-3.21
α -U ^a	0.676 (XAS)	-0.190		$5f^3$				
	0.686 (EELS)			$5f^3$				

^aTaken from Ref. 30.

independently of the U and Fe thickness. This confirms the conclusion reached independently from the Fe K edge XMCD.

3. Dependence of the XMCD signal on the U layer thickness and temperature

In Fig. 5(b) we show the XMCD signal for different U thicknesses, while keeping the Fe thickness constant (~ 32 Å). As we have noted above, for Fe thicknesses between 29 and 34 Å, the intensity of the XMCD signal at the Fe K edge is the same, implying that the Fe layers carry a similar average magnetic moment. This is important in order to compare the induced polarization of the U atoms. We note first that the XMCD spectra at both the M_5 and M_4 edges are

similar in shape; their amplitudes decrease when the U thickness increases. From this observation we can directly conclude that the induced magnetization profile of the U $5f$ magnetic moments is not constant within the U layers. The decrease of the XMCD signal with increasing U layer thickness suggests that only those U atoms located near the interface are extensively polarized and the layers further away from the interface have the *opposite* polarization.

Consideration of the XMCD at 10 and 300 K (Fig. 6) for the two U/Fe multilayers, (a) U₁₈/Fe₃₄ and (b) U₂₆/Fe₂₉, confirms that the XMCD signal at the U $M_{4,5}$ edges is due to Fe($3d$)-U($6d$)-U($5f$) hybridization. At 300 K, the XMCD signal at both M_5 and M_4 edges is reduced by approximately 13% and 27%, respectively, for the two multilayers. For the

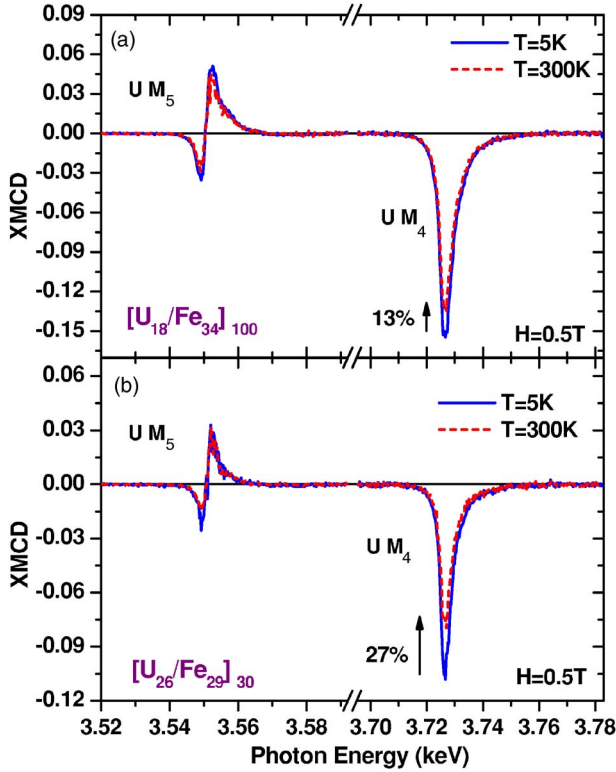


FIG. 6. (Color online) XMCD spectra at the M_5 (3.55 keV) and M_4 (3.72 keV) edges of U in two different U/Fe multilayers (a) $[U_{18}/Fe_{34}]_{100}$ and (b) $[U_{26}/Fe_{29}]_{30}$ measured at 10 K (solid blue line) and 300 K (broken red line) under 0.5 T. Compared to low temperature, a reduction of the XMCD signal at both $M_{4,5}$ edges of $\sim 13\%$ and $\sim 27\%$ is observed at room temperature for the two (a) and (b) multilayers, respectively.

U_{40}/Fe_9 multilayer, the XMCD signal is reduced by 60%. If this signal arose from a UFe_2 alloy located at the interface, we would not expect any XMCD signal at 300 K, since the T_C for UFe_2 is ~ 160 K. A rough estimate from the temperature dependence of the XMCD signal suggests the T_C for multilayers with thin Fe layers (9 Å) is ~ 400 K, which is much lower than the T_C of bulk Fe, due to finite-size, low-dimensionality, and hybridization effects.³⁴ For the thick Fe layers (~ 32 Å), since T_C is closer to the bulk value of Fe, a smaller reduction of the XMCD signal is observed.

4. Element-specific hysteresis curves

To ensure complete magnetic saturation, element-specific hysteresis curves were performed at the maximum of the $U M_4$ edge XMCD signal at 5 K for U_{18}/Fe_{34} and at 300 K for U_{26}/Fe_{29} multilayers (Fig. 7). If the magnetic moments are purely induced, as for example in Ni/Pt multilayers,³⁵ the hysteresis behavior of the uranium should follow the magnetization behavior of the Fe layers. For the two U/Fe multilayers considered, nearly square loops were observed with similar coercive fields of about 0.013 T for the sample with thinner U layers (18 Å) and thicker U layers (26 Å) for similar Fe thickness. The small coercive field and saturation field are in good accord with the ones observed in ferromagnetic

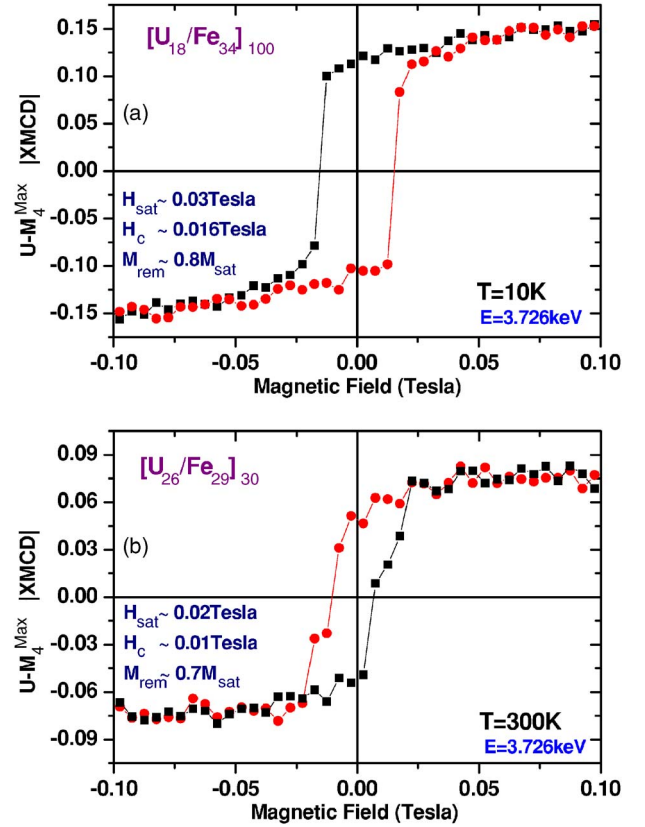


FIG. 7. (Color online) Typical hysteresis curves measured at the maximum XMCD signal at the $U M_4$ edge at 10 K with the field parallel to the plane of the multilayer. As an illustration, two different U/Fe multilayers (a) $[U_{18}/Fe_{34}]_{100}$ and (b) $[U_{26}/Fe_{29}]_{30}$ are presented. The hysteresis curves are nearly independent of the U thickness.

thin films. These results confirm that the moment on the U atoms is an induced effect.

5. Orbital and spin magnetic moments

One of the great advantages of the XMCD technique is that it allows information to be obtained about the orbital and spin magnetic moments of a given electronic shell of an atom using magneto-optical sum rules.^{36,37} Since these sum rules involve only the integrated intensity of the absorption and dichroic spectra, the results are independent of the shape of the XMCD spectra. The sum rules for the XMCD spectra at the uranium $M_{4,5}$ edges, considering only $3d \rightarrow 5f$ transitions (we neglect $3d \rightarrow 6p$ dipolar transitions), can be written as

$$\langle L_z \rangle = \frac{3n_h^{5f} \int_{M_5+M_4} \Delta\mu(E) dE}{\int_{M_5+M_4} [\mu^+(E) + \mu^-(E) + \mu^{iso}(E)] dE}, \quad (5)$$

$$\langle S_Z^{eff} \rangle = \frac{3n_h^{5f}}{4} \frac{2 \int_{M_5} \Delta\mu(E)dE - 3 \int_{M_4} \Delta\mu(E)dE}{\int_{M_5+M_4} [\mu^+(E) + \mu^-(E) + \mu^{iso}(E)]dE}, \quad (6)$$

where μ^\pm are the absorption coefficients at the $M_{4,5}$ edges for right and left circularly polarized x rays. The corresponding dichroism is $\Delta\mu = \mu^+ - \mu^-$, and μ^{iso} is the isotropic absorption coefficient for unpolarized x rays, where $\mu^{iso} = (\mu^+ + \mu^-)/2$. The number of $5f$ holes is n_h^{5f} , which is equal to $(14 - n_e^{5f})$, where n_e^{5f} is the number of $5f$ electrons and E is the photon energy $\hbar\omega$.

The XMCD recorded at the $U M_{5,4}$ edges allows the determination of the ground state expectation values of the z component of the $5f$ orbital magnetic moment $\langle L_Z \rangle$ and the $5f$ effective spin magnetic moment $\langle S_Z^{eff} \rangle$ where

$$\langle S_Z^{eff} \rangle = \langle S_Z \rangle + 3\langle T_Z \rangle. \quad (7)$$

Here $\langle T_Z \rangle$ is the expectation value of the z projection of the magnetic dipole operator of the $5f$ shell. The orbital and spin contributions to the magnetic moments deduced from the sum rules^{36,37} are summarized in Table II, taking the n_h^{5f} and $\langle T_Z \rangle$ values corresponding to each of the two uranium valence states $5f^2$ (U^{4+} : $\langle T_Z \rangle = 1.16\langle S_Z \rangle$) and $5f^3$ (U^{3+} : $\langle T_Z \rangle = 0.62\langle S_Z \rangle$).³⁸ We have also considered the case where $\langle T_Z \rangle = 0$. For the case of a polycrystalline sample, e.g. U in U/Fe multilayers where the uranium possesses a strong spin-orbit coupling,³⁹ the $\langle T_Z \rangle$ contribution may be smaller than that derived on the basis of a purely atomic picture,³⁸ within the sum-rule approximations.³⁷ For US, which is known to be highly anisotropic, the $\langle T_Z \rangle$ contribution is important⁴⁰ and its magnitude, found by comparing the results of XMCD and polarized neutron diffraction, is in fair agreement with sum rule considerations³⁸ and theoretical (Hartree-Fock) values.⁴¹ The fact that the $\langle T_Z \rangle$ contribution is small may be justified by the shape of the XMCD signal. Yaouanc *et al.*²⁶ have calculated within the intermediate coupling scheme the shape of the XMCD signal at the $M_{5,4}$ edges of U for different electronic configurations taking into account crystal-field interactions. Despite an oversimplified model used to compute the dichroism shape, the best agreement, especially for the XMCD signal at the M_5 edge, is found when this interaction is considered, as was also found for UPd_2Al_3 . As a consequence, because of the strong interaction of the uranium $5f$ electrons with their environment, the ratio $R_T = \langle T_Z \rangle / \langle S_Z \rangle$ for $n_e^{5f} = 2$ and $n_e^{5f} = 3$ is around 0.4 and nearly zero, respectively.²⁶

Moreover, in the case of UFe_2 , a nearly total cancellation of the spin and orbital magnetic moments leads to a vanishing total U $5f$ magnetic moment. A good agreement with polarized neutron diffraction and theoretical predictions is obtained if $\langle T_Z \rangle$ is assumed to be equal to zero.²⁴ Indeed, the delocalization of the electrons, which takes place in itinerant ferromagnets, can strongly reduce $\langle T_Z \rangle$ with respect to its atomic value. Using *ab initio* calculations to determine the U magnetic moments in a UAs/Co multilayer,⁴² the magnitude

of the magnetic-dipole term $\langle T_Z \rangle$ was found to be small. The $\langle T_Z \rangle$ contribution is important because it affects directly the sign of the total U $5f$ magnetic moment with respect to that of the iron. Indeed, taking into account the atomiclike, non-zero $\langle T_Z \rangle$ contribution results in a U $5f$ induced orbital magnetic moment larger than the spin moment. The total induced (U $5f$) moment is then coupled *parallel* to the Fe magnetic moment (which points along the external magnetic field). As shown in Table II, this result is independent of the U or Fe thickness.

In contrast, if the $\langle T_Z \rangle$ contribution is equal to zero or negligible, the situation is very different; the spin magnetic moment (U $5f$) is larger than the orbital moment and the total induced moment is then *antiparallel* to that of the iron. The $\langle T_Z \rangle$ term affects only the determination of the spin magnetic moment. The sign and magnitude of the orbital magnetic moment, however, are independent of this term. From these considerations, it is clear that a knowledge of the $\langle T_Z \rangle$ term is important for U atoms carrying an induced magnetic moment. From the experimental XMCD spectrum it is not possible to discriminate between these two cases. However, the electronic and magnetic properties of U films and U/Fe multilayers, within the framework of the density functional theory, have recently been reported.⁴³ These calculations considered idealized multilayers, consisting of a monolayer of U, oriented [001], and three monolayers of Fe, oriented [110], and show that the U layer is magnetic with the direction of the U moments opposite to that of the Fe moments. Our results agree with these calculations if we assume that the dipole magnetic term $\langle T_Z \rangle$ is negligible.

Finally, we are not able to determine the uranium electronic configuration precisely. For simplicity, we will assume that the valence state is $5f^{2.5}$ for U in all U/Fe multilayers and consider that $\langle T_Z \rangle = 0$ in the following discussion. Although the number of $5f$ holes is not exactly known but oscillates between $n_h^{5f} = 12$ and 11 as a function of the U thickness, the differences in applying the sum rule, which depends linearly on the number of $5f$ holes, will be only a 5% deviation if one assumes a $5f^{2.5}$ electronic configuration for all the U/Fe multilayers. As shown in Fig. 8, the induced $5f$ spin and orbital magnetic moments are largest for the thinnest U layer (9 Å), $-0.31(5)\mu_B$ and $0.18\mu_B$, respectively, giving a maximum average induced moment in the U layers of $0.13\mu_B$ directed antiparallel to the Fe moment. For thicker U layers, the average induced magnetic moment decreases. The magnetization profile is consequently not constant but varies from the interface to the center of the layer. The value of the orbital to spin moment ratio appears roughly constant across the whole series (lower panel of Fig. 8) with a value of about -0.55 . The assumption that $\langle T_Z \rangle = 0$ is, of course, consistent with a large reduction of the orbital moment, so that this ratio of orbital to spin moments is consistent with strong hybridization between the U $5f$ and Fe $3d$ states.⁴⁴

6. Profile of total induced magnetic moment

Experiments on four different multilayers of almost identical Fe thickness, U_9/Fe_{34} , U_{18}/Fe_{34} , U_{26}/Fe_{29} , and U_{32}/Fe_{30} , may be analyzed to give the profile across the U

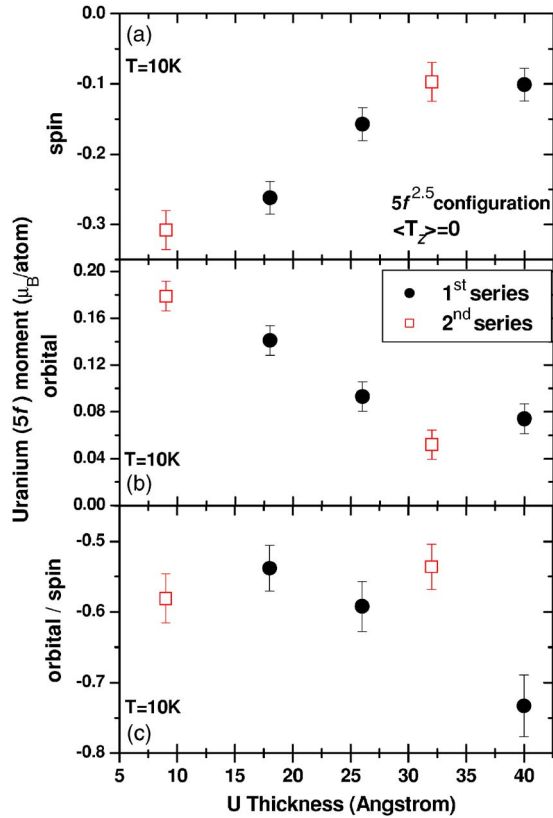


FIG. 8. (Color online) U ($5f$) spin- (a) and orbital- (b) induced magnetic moments averaged over the U layers for U/Fe multilayers at 10 K. The ratio of orbital to spin magnetic moment is shown on the bottom panel (c). The magnetic moments have been determined via the XMCD sum rules for a $5f$ U valence state of 2.5 (assuming a value of $\langle T_Z \rangle = 0$).

layers, provided that this profile depends only on the layer thickness, and not on other factors. We may extract the profile of the induced U moment by an analysis that considers “slices” of thickness 4.5 \AA across the thickest U layer of 36 \AA . One has to assume for this that the U slices do not interact with each other, that the structural properties (roughness, interface mixing, and strain) are the same for the four multilayers, and that the magnetism at both U/Fe and Fe/U

interfaces is equivalent. Further, for this model we assume $\langle T_Z \rangle = 0$ and a $5f^{2.5}$ electronic configuration. We show the results in Fig. 9 in terms of the moments induced in each atomic slice of U. Note that the sign is with respect to that of the Fe $3d$ moment, which for this thickness of Fe ($\sim 32 \text{ \AA}$) is about $1\mu_B$.¹⁰ By assumption, this curve is symmetrical across the Fe/U and U/Fe interfaces (which may not be the case in practice once the location of the nonmagnetic amorphous Fe is established) and is characterized by a U moment of $\sim -0.12\mu_B$ at the interface, decreasing within the U part of the multilayer to a positive value [by the third atomic layer ($\sim 15 \text{ \AA}$)].

We can compare the U moment profile of Fig. 9 with that deduced for the Ce moments in Ce/Fe multilayers.^{45–47} In the case of Ce and compounds the $5d$ polarization is often similar in magnitude to that of the $4f$ (since the latter comes from a single $4f$ electron). For both the $5d$ (L edges) (Refs. 40 and 41) and $4f$ (M edges) (Ref. 47) electrons, the sign of the signal at the Ce/Fe interface is antiparallel to that of the Fe layer. In Ce the $4f$ moment is small and the orbital moment is even smaller, so the total $4f$ moment, which is dominated by the spin moment, is induced parallel to the conduction states. The situation appears very similar for the U/Fe multilayers, but it must be remembered that we have assumed a $\langle T_Z \rangle = 0$ to arrive at this conclusion. Whereas this is certainly justified in the case of Ce $5d$ conduction states, the same may not be true of U $5f$ states. This emphasizes the need for further experiments and theory on the actinide materials.

IV. CONCLUSIONS

The XMCD experiments at the Fe K edge have shown that the Fe moments in U/Fe multilayers are similar to those of elemental bcc Fe. There is evidence for a *change* in the electronic structure (as measured by the XANES signal, Fig. 1(a), for thin Fe layers; we associate this with the dominance of nonmagnetic (presumably amorphous) Fe in the thinnest layers. Amorphous U-Fe alloys are known to exist^{48,49} and for high U content, which would be expected near the U layer, would be nonmagnetic. A detailed structural model for these interfaces is still lacking and presumably complex.

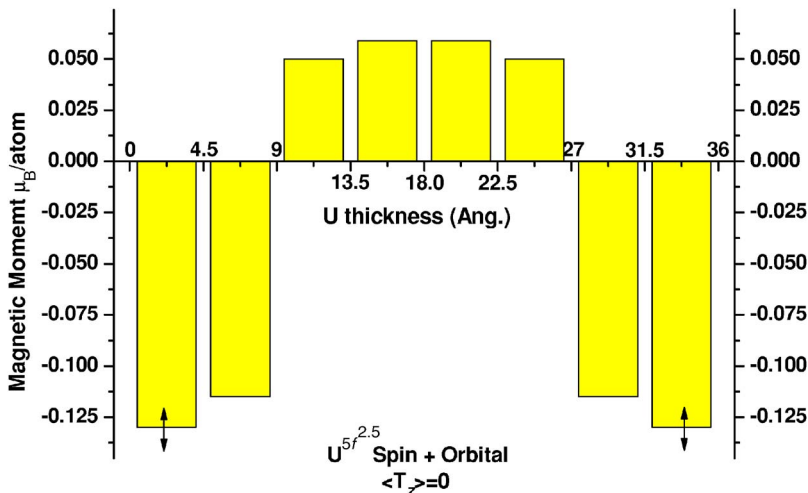


FIG. 9. (Color online) Induced U magnetic moment (spin+orbital) profile for a model U_{36}/Fe_{32} multilayer assuming a $5f$ U valence state of 2.5 and $\langle T_Z \rangle = 0$. See discussion in Sec. III B 6

This is in agreement with the interpretation of the Mössbauer experiments reported earlier.¹⁰ The moments in the Fe layers increase approximately linearly (Fig. 4) up to the maximum thickness examined here of 34 Å, at which thickness the polarized-neutron reflectivity experiments¹⁰ show that the Fe moments are $\sim 1\mu_B$. The absorption and XMCD signals at *both* the Fe (Fig. 3) and U edges (Fig. 5) argue against the presence of any significant amount of the compound UFe₂; a conclusion also reached by the interpretation of the Mössbauer spectra.⁹

XMCD at the U *M* edges (Fig. 5) establishes that, in all the multilayers studied, there are induced moments present on the U atoms. The fact that the largest XMCD signals are found in the thinnest U layers strongly suggests that the U moments are (a) not uniform across the layers and (b) greatest at the interfaces, and oscillate within the uranium layer. This conclusion is independent of any assumption about $\langle T_Z \rangle$, and is simply a consequence of seeing a smaller signal in XMCD as the uranium thickness is increased beyond ~ 20 Å. Assuming a symmetric profile of the layers, this suggests that the signal within the U layers changes sign after about 10 Å, i.e., four atomic layers of uranium. The exact form of the profile, and most importantly its sign with respect to the dominant Fe moment, does depend on $\langle T_Z \rangle$.

The electronic structure of the induced U signals is different from that found in (amorphous UAs)/Co multilayers examined previously,⁷ which is not surprising considering that the U atoms in amorphous UAs are more separated than in the elemental form produced here, and the material itself is ferromagnetic. The temperature dependence (Fig. 6) and the element-specific hysteresis loops (Fig. 7) at the U *M*₄ edge are both consistent with the idea that the U moment is completely induced, i.e., depends on the Fe moment. The ratio of the orbital to spin values (Table II and Fig. 8), as deduced by XMCD, is (-0.55 ± 0.1) , under the assumption that the dipole magnetic term $\langle T_Z \rangle$ is negligible. The drop in polarization of the U atoms on moving away from the Fe interface is reminiscent of the predicted polarization of elemental α -U at its surface,⁵⁰ where the polarization dies rapidly on going into the bulk, as well as the results of calculations for similar multilayers containing uranium.^{42,43}

ACKNOWLEDGMENTS

The authors would like to thank A. V. Andreev for providing us with a single crystal of UFe₂. R.S. acknowledges the financial support by EPSRC. A.M.B. is grateful for the support of ORS.

*Also at Department of Physics, University of Liverpool, Liverpool L69 7ZE, United Kingdom.

¹I. K. Schuller, S. Kim, and C. Leighton, *J. Magn. Magn. Mater.* **200**, 571 (1999).

²R. E. Parra and J. W. Cable, *J. Appl. Phys.* **50**, 7522 (1979).

³*Spin-Orbit-Influenced Spectroscopies of Magnetic Solids*, edited by H. Ebert and G. Schütz, Lecture Notes in Physics Vol. 466 (Springer, Berlin, 1996), and references therein.

⁴P. Pouloupoulos, A. Scherz, F. Wilhelm, H. Wende, and K. Baberschke, *Phys. Status Solidi A* **189**, 293 (2002).

⁵P. Santini, R. Lémanski, and P. Erdős, *Adv. Phys.* **48**, 537 (1999).

⁶P. Fumagalli, T. S. Plaskett, D. Weller, T. R. McGuire, and R. J. Gambino, *Phys. Rev. Lett.* **70**, 230 (1993).

⁷N. Kernavanois, D. Mannix, P. Dalmás de Réotier, J.-P. Sanchez, A. Yaouanc, A. Rogalev, G. H. Lander, and W. G. Stirling, *Phys. Rev. B* **69**, 054405 (2004).

⁸S. D. Brown, A. Beesley, A. Herring, D. Mannix, M. F. Thomas, P. Thompson, L. Bouchenoire, S. Langridge, G. H. Lander, W. G. Stirling, A. Mirone, R. C. C. Ward, M. R. Wells, and S. W. Zochowski, *J. Appl. Phys.* **93**, 6519 (2003).

⁹A. M. Beesley, M. F. Thomas, A. D. F. Herring, R. C. C. Ward, M. R. Wells, S. Langridge, S. D. Brown, S. W. Zochowski, L. Bouchenoire, W. G. Stirling, and G. H. Lander, *J. Phys.: Condens. Matter* **16**, 8491 (2004).

¹⁰A. M. Beesley, S. W. Zochowski, M. F. Thomas, A. D. F. Herring, S. Langridge, S. D. Brown, R. C. C. Ward, M. R. Wells, R. Springell, W. G. Stirling, and G. H. Lander, *J. Phys.: Condens. Matter* **16**, 8507 (2004).

¹¹A. M. Beesley, Ph.D. thesis, University of Liverpool, 2005.

¹²S. Langridge, ISIS, Rutherford Appleton Laboratory, U.K., <http://www.rl.ac.uk/largescales/>

¹³A. Rogalev, J. Goulon, C. Goulon-Ginet, and C. Malgrange, in *Magnetism and Synchrotron Radiation*, edited by E. Beaurepaire, F. Scheurer, G. Krill, and J.-P. Kappler, Lecture Notes in Physics Vol. 565 (Springer, Berlin, 2001).

¹⁴J. Goulon, C. Goulon-Ginet, R. Cortes, and J. M. Dubois, *J. Phys. (Paris)* **43**, 539 (1982); L. Tröger, D. Arvanitis, K. Baberschke, H. Michaelis, U. Grimm, and E. Zschech, *Phys. Rev. B* **46**, 3283 (1992); P. Pfalzer, J.-P. Urbach, M. Klemm, S. Horn, M. L. denBoer, A. I. Frenkel, and J. P. Kirkland, *ibid.* **60**, 9335 (1999).

¹⁵E. Sobczak, Y. Swilem, N. N. Dorozhkinc, R. Nietubyc, P. Dlużewska, and A. Ślawska-Waniewska, *J. Alloys Compd.* **328**, 57 (2001).

¹⁶H. J. Gotsis and P. Strange, *J. Phys.: Condens. Matter* **6**, 1409 (1994).

¹⁷M. S. S. Brooks and B. Johansson, in *Spin-Orbit Influenced Spectroscopies of Magnetic Solids*, edited by H. Ebert and G. Schütz, Lecture Notes in Physics Vol. 466 (Springer, Berlin, 1996), p. 211.

¹⁸J.-I. Igarashi and K. Hirai, *Phys. Rev. B* **50**, 17820 (1994).

¹⁹H. Ebert, *Rep. Prog. Phys.* **59**, 1665 (1996).

²⁰J. Chaboy, M. A. Laguna-Marco, M. C. Sánchez, H. Maruyama, N. Kawamura, and M. Suzuki, *Phys. Rev. B* **69**, 134421 (2004).

²¹M. L. Fdez-Gubieda, A. García-Arribas, J. M. Barandiarán, R. López Antón, I. Orue, P. Gorria, S. Pizzini, and A. Fontaine, *Phys. Rev. B* **62**, 5746 (2000).

²²S. Komura, Y. Hamaguchi, M. Sakamoto, and N. Kunitomi, *J. Phys. Soc. Jpn.* **16**, 1486 (1961).

²³A. V. Andreev, A. V. Deryagin, R. Z. Levitin, A. S. Markosyan, and M. Zeleny, *Phys. Status Solidi A* **52**, K13 (1979).

²⁴M. Finazzi, P. Sainctavit, A.-M. Dias, J.-P. Kappler, G. Krill, J.-P. Sanchez, P. Dalmás de Réotier, A. Yaouanc, A. Rogalev, and J.

- Goulon, Phys. Rev. B **55**, 3010 (1997).
- ²⁵A. Koizumi, M. Takagaki, M. Suzuki, N. Kawamura, and N. Sakai, Phys. Rev. B **61**, R14909 (2000).
- ²⁶A. Yaouanc, P. Dalmas de Réotier, G. van der Laan, A. Hiess, J. Goulon, C. Neumann, P. Lejay, and N. Sato, Phys. Rev. B **58**, 8793 (1998).
- ²⁷P. Dalmas de Réotier, A. Yaouanc, G. van der Laan, N. Kernavanois, J.-P. Sanchez, J. L. Smith, A. Hiess, A. Huxley, and A. Rogalev, Phys. Rev. B **60**, 10606 (1999).
- ²⁸V. N. Antonov, B. N. Harmon, and A. N. Yaresko, Phys. Rev. B **68**, 214424 (2003).
- ²⁹A. N. Yaresko, V. N. Antonov, and B. N. Harmon, Phys. Rev. B **68**, 214426 (2003).
- ³⁰G. van der Laan, K. T. Moore, J. G. Tobin, B. W. Chung, M. A. Wall, and A. J. Schwartz, Phys. Rev. Lett. **93**, 097401 (2004).
- ³¹J. G. Tobin, K. T. Moore, B. W. Chung, M. A. Wall, A. J. Schwartz, G. van der Laan, and A. L. Kutepov, Phys. Rev. B **72**, 085109 (2005).
- ³²K. T. Moore, G. van der Laan, R. G. Haire, M. A. Wall, and A. J. Schwartz, Phys. Rev. B **73**, 033109 (2006).
- ³³K. T. Moore, M. A. Wall, A. J. Schwartz, B. W. Chung, S. A. Morton, J. G. Tobin, S. Lazar, F. D. Tichelaar, H. W. Zandbergen, P. Soderlind, and G. van der Laan, Philos. Mag. **84**, 1039 (2004).
- ³⁴P. J. Jensen, H. Dreyssé, and K. H. Bennemann, Europhys. Lett. **18**, 463 (1992).
- ³⁵P. Pouloupoulos, F. Wilhelm, Z. Li, A. Scherz, H. Wende, K. Baberschke, M. Angelakeris, N. K. Flevaris, A. Rogalev, and N. B. Brookes, J. Magn. Magn. Mater. **272**, 317 (2004).
- ³⁶B. T. Thole, P. Carra, F. Sette, and G. van der Laan, Phys. Rev. Lett. **68**, 1943 (1992).
- ³⁷P. Carra, B. T. Thole, M. Altarelli, and X. Wang, Phys. Rev. Lett. **70**, 694 (1993).
- ³⁸G. van der Laan and B. T. Thole, Phys. Rev. B **53**, 14458 (1996).
- ³⁹J. Stöhr and H. König, Phys. Rev. Lett. **75**, 3748 (1995).
- ⁴⁰A. Bombardi, N. Kernavanois, P. Dalmas de Réotier, G. H. Lander, J. P. Sanchez, A. Yaouanc, P. Burllet, E. Lelièvre-Berna, A. Rogalev, O. Vogt, and K. Mattenberger, Eur. Phys. J. B **21**, 547 (2001).
- ⁴¹T. Shishidou, T. Oguchi, and T. Jo, Phys. Rev. B **59**, 6813 (1999).
- ⁴²M. Komelj and N. Stojić, Phys. Rev. B **71**, 052410 (2005).
- ⁴³A. Laref, E. Sasioglu, and L. M. Sandratskii, J. Phys.: Condens. Matter **18**, 4177 (2006).
- ⁴⁴G. H. Lander, M. S. S. Brooks, and B. Johansson, Phys. Rev. B **43**, 13672 (1991).
- ⁴⁵L. Sève, N. Jaouen, J. M. Tonnerre, D. Raoux, F. Bartolomé, M. Arend, W. Felsch, A. Rogalev, J. Goulon, C. Gautier, and J. F. Bézar, Phys. Rev. B **60**, 9662 (1999).
- ⁴⁶N. Jaouen, J. M. Tonnerre, D. Raoux, E. Bontempi, L. Ortega, M. Muenzenberg, W. Felsch, A. Rogalev, H. A. Dürr, E. Dudzik, G. van der Laan, H. Maruyama, and M. Suzuki, Phys. Rev. B **66**, 134420 (2002).
- ⁴⁷N. Jaouen, J. M. Tonnerre, D. Raoux, M. Muenzenberg, W. Felsch, A. Rogalev, N. B. Brooks, H. Dürr, and G. van der Laan, Acta Phys. Pol. B **34**, 1403 (2003).
- ⁴⁸P. P. Freitas, T. S. Plaskett, and T. R. McGuire, J. Appl. Phys. **63**, 3746 (1988).
- ⁴⁹S. J. Poon, A. J. Drehman, K. M. Wong, and A. W. Clegg, Phys. Rev. B **31**, 3100 (1985).
- ⁵⁰N. Stojic, J. W. Davenport, M. Komelj, and J. Glimm, Phys. Rev. B **68**, 094407 (2003).